



Published in final edited form as:

*Glia*. 2017 July ; 65(7): 1043–1058. doi:10.1002/glia.23142.

## Astrocyte-Specific Insulin-Like Growth Factor-1 Gene Transfer in Aging Female Rats Improves Stroke Outcomes

Andre Okoreeh, Shameena Bake, and Farida Sohrabji

Women's Health in Neuroscience Program, Neuroscience and Experimental Therapeutics, Texas A&M College of Medicine, Bryan TX 77807

### Abstract

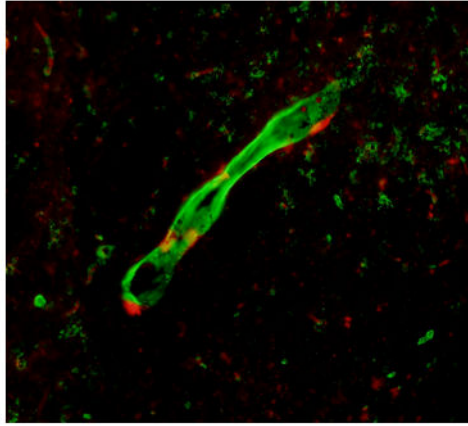
Middle aged female rats sustain larger stroke infarction and disability than younger female rats. This older group also shows age-related reduction of insulin like growth factor (IGF)-1 in serum and in astrocytes, a cell type necessary for post stroke recovery. To determine the impact of astrocytic IGF-1 for ischemic stroke, these studies tested the hypothesis that gene transfer of IGF-1 to astrocytes will improve stroke outcomes in middle aged female rats. Middle aged (10–12 month old), acyclic female rats were injected with recombinant adeno-associated virus serotype 5 (AAV5) packaged with the coding sequence of the human (h)IGF-1 gene downstream of an astrocyte-specific promoter GFAP (AAV5-GFP-hIGF-1) into the striatum and cortex. The AAV5-control consisted of an identical shuttle vector construct without the hIGF-1 gene (AAV5-GFAP-control). Six to eight weeks later, animals underwent transient (90 mins) middle cerebral artery occlusion via intraluminal suture. While infarct volume was not altered, AAV5-GFAP-hIGF-1 treatment significantly improved blood pressure and neurological score in the early acute phase of stroke (2 days) and sensory-motor performance at both the early and late (5 days) acute phase of stroke. AAV5-GFAP-hIGF-1 treatment also reduced circulating serum levels of GFAP, a biomarker for blood brain barrier permeability. Flow cytometry analysis of immune cells in the brain at 24h post stroke showed that AAV5-GFAP-hIGF-1 altered the type of immune cells trafficked to the ischemic hemisphere, promoting an anti-inflammatory profile. Collectively, these studies show that targeted enhancement of IGF-1 in astrocytes of middle-aged females improves stroke-induced behavioral impairment and neuroinflammation.

### Graphical Abstract

---

Correspondence to: Farida Sohrabji, Ph.D., Texas A&M College of Medicine, Neuroscience and Experimental Therapeutics, MREB 4102 State Hwy 47, Bryan TX 77807, Ph: 979-436-0335, Sohrabji@medicine.tamhsc.edu.

Conflict of Interest: The authors declare no competing financial interests



### Keywords

blood brain barrier; M1/M2 activation; sensory motor tasks; middle cerebral artery occlusion

---

## INTRODUCTION

Ischemic stroke is the 5<sup>th</sup> leading cause of mortality, and the major cause of long term disability, especially among the elderly (Mozaffarian et al. 2015). Loss of nutrients, due to occlusion of a cerebral vessel, initiates a sequence of damaging events within neurons including rapid failure of ATP-dependent processes (Rossi et al. 2007), increased release of glutamate and calcium (Bano et al. 2005), and a loss of cellular integrity (Lo et al. 2003). Transient ischemia, followed by reperfusion, also increases permeability of the blood brain barrier and increases brain trafficking of cytotoxic cells and proteins. Non-neuronal cells such as astrocytes and endothelial cells, that are critical constituents of the blood brain barrier, also play a critical role in ischemic injury and repair (Panickar and Norenberg 2005; Posada-Duque et al. 2014).

Astrocytes are well positioned for neuroprotection during ischemia. They provide growth factors (Karki et al. 2014), clear glutamate (Olsen and Sontheimer 2008), preserve blood brain barrier function (Abbott et al. 2006) (Cekanaviciute and Buckwalter 2016), interact with the immune system (Xie and Yang 2015), combat oxidative stress (Xu et al. 2010) and produce functional extracellular mitochondria to support neuronal viability (Hayakawa et al. 2016). Astrocytes are less vulnerable to ischemic injury than neurons (Dienel and Hertz 2005) and have a greater capacity for self-preservation (Allaman et al. 2011), indicating that these cells may play a crucial role in post-stroke recovery.

The ability of astrocyte's to promote neuroprotection deteriorates with age, when the CNS is more prone to disease pathology particularly stroke (reviewed in Chisholm *et al.*, 2015). Proliferation of reactive astrocytes after injury is greater (Topp et al. 1989) and persists longer in the aged brain (Manwani et al. 2011) and results in accelerated glial scar formation in this group (Badan et al. 2003). Aged reactive astrocytes exhibited an upregulation of genes associated with inflammation and scar formation as compared to adult astrocytes

(Buga et al. 2008). Moreover, aging also affects astrocytic functions critical for stroke recovery such reduced glutamate uptake capacity in aging male rats (Latour et al. 2013) and in middle aged female rats (Lewis et al. 2012). Similarly, while astrocytes normally release a variety of trophic factors that promote neuronal survival and curb CNS degeneration (Ridet et al. 1997) including IGF-1 and VEGF (Chisholm and Sohrabji 2016), these secretions decrease with age (Bhat et al. 2012; Lewis et al. 2012). The loss of IGF-1 observed in aging astrocytes may result in more severe stroke outcomes observed in middle aged female rats.

IGF-1 plays an important role in development, cell differentiation, neuronal plasticity, and cell survival of the nervous system (Bondy and Cheng 2004). IGF-1 also reduces cell death in a variety of experimental neurologic disease models, such Parkinson's (Ayadi et al. 2016) traumatic brain injury (Madathil et al. 2013), and spinal cord injury (Utada et al. 2015). With age, plasma levels of IGF-1 decrease in many species and in female rats, this decrease is seen as early as middle age, when stroke induced infarction is more severe as compared to young females (Selvamani and Sohrabji, 2010). Intracerebroventricular (ICV) treatment with IGF-1 post-stroke has been reported to decrease infarct volumes in this group (Bake *et al.*, 2014), suggesting that the loss of IGF-1 with age may underlie the more severe stroke outcomes seen in middle-aged females.

In view of the crucial role that astrocytes play in brain injury along with the age-related loss of IGF-1 in middle-aged females, we hypothesize that worse stroke outcomes in this age group is due to reduced availability of astrocytic IGF-1, and that increasing IGF-1 expression in aging astrocytes will improve post-stroke outcomes in this group. To test this hypothesis, middle-aged females were injected with recombinant human (h)IGF-1 placed downstream of the GFAP promoter and packaged in recombinant adeno-associated virus serotype 5 (AAV5) or with control construct. Following stroke, animals were tested for behavioral impairments, extent of infarction, and neuroinflammation. Our studies show that gene transfer of IGF-1 to astrocytes significantly improves stroke-induced behavioral impairment, without reducing infarct volume, and further reduces neuroinflammation in a model of ischemia reperfusion.

## MATERIALS AND METHODS

### Animals

Female Sprague Dawley (SD) rats were purchased as retired breeders (10 – 12 months; weight range 325 – 350 g) from Envigo Laboratories. This group met our previously established criteria for reproductive senescence: briefly, at least five successful pregnancies and current acyclicity as defined by vaginal cytology assessed via daily vaginal smears (Jeziarski and Sohrabji 2001). All animals were housed in an AAALAC-approved facility, maintained on a constant photoperiod (12-hour light/dark cycles), and fed ad libitum with laboratory chow (Harlan Teklad 8604) and water. All animal procedures were performed in accordance with the National Institutes of Health guidelines for the humane care of laboratory animals and were approved by the Institutional Animal Care Committee and the Institutional Biosafety Committee. A total of 112 animals were used in this study.

## Adenovirus constructs

Recombinant adeno associated virus serotype 5 (AAV5) was packaged (Signagen, MD) with the ORF of the human (h)IGF-1 gene downstream of the astrocyte-specific promoter, GFAP (AAV5-GFAP-hIGF-1; see Figure 1). The construct also contained the mCherry reporter gene under the CMV minimal promoter to visually detect transfected cells. The control construct consisted of an identical shuttle vector without the hIGF-1 gene (AAV5-GFAP-control).

## Surgical procedures

**AAV5 injections**—Animals were anesthetized (ketamine: 87 mg/kg; xylazine: 13 mg/kg) and placed in a stereotaxic instrument (David Kopf Instruments). Two small holes were drilled into the skull at the following coordinates relative to bregma. For striatum: +0.9 mm anterior posterior, +3.6 mm medial lateral, and a depth of 6.5 mm relative to the dura. For cortex: +0.9 mm anterior posterior, +5.5 mm medial lateral, and a depth of 6.0 mm relative to the dura. In each case, a needle, attached to a Hamilton syringe was lowered to the required depth and AAV5 was delivered slowly to the parenchyma at the rate of 0.02  $\mu\text{L}/30$  seconds for a total of 3.5  $\mu\text{L}$ . All animals received one injection each into both the right striatum and right cortex of either the AAV5-GFAP-hIGF-1 construct or the AAV5-GFAP-control construct (Figure 1C). Two concentrations of AAV5 were used:  $2.5 \times 10^{11}$  viral particles (VP)/mL (low dose) and  $2.5 \times 10^{12}$  (VP)/mL (high dose). Animals were allowed to recover for 6–8 weeks after injections to allow full integration of the viral particles.

## Middle cerebral artery occlusion (MCAo)

Animals were subjected to middle cerebral artery occlusion (MCAo) via intraluminal suture using our previous procedures (Bake et al. 2016; Bake et al. 2014). Briefly, rats were anesthetized with isoflurane and maintained at 37°C on heating pads in dorsal recumbency. The neck region was shaved and disinfected and a ventral midline incision was made on the skin. Superficial fascia on the right side of the neck was dissected and the underlying muscles were bluntly dissected to expose the right common carotid (CCA), external (ECA), and internal carotid (ICA) arteries. The ECA was separated from the vagus nerve and tied off distally with silk sutures after cauterizing the small branches. Microsurgical clamps were placed on the CCA and ICA. A loose tie was placed on the ECA, and the free stump of ECA was aligned with the ICA. Twenty-two mm of suture of the appropriate size with a silicon-coated round tip (Doccol Corp., CA) was inserted into ICA lumen through a small nick on the ECA between the two ties. The suture was advanced along the ICA until it reached the origin of the MCA (~20 mm of suture) and secured in position with nylon ties. The intraluminal suture was maintained for 90 min and then withdrawn. Tissue perfusion rate was monitored using Laser-Doppler Flowmetry (Moor Instruments, UK) and the perfusion index was calculated for both ischemic and reperfusion time points. MCAo resulted in an 80% reduction of blood flow compared to the pre-occlusion rate and re-perfusion restored the perfusion index back to pre-occlusion levels. In a subset of animals, a permanent (p)MCAo was performed, where the suture was maintained in place for the duration of the experiment. All animals were carefully monitored after surgery and terminated 2 days (early acute phase) or 5 days (late acute phase) after ischemia.

### Confirmation of AAV5 localization

A subset of AAV5-GFAP-control and AAV5-GFAP-hIGF-1 injected animals were terminated 2 days after MCAo and processed for histological analyses to determine uptake of the AAV5 construct. Animals were perfused transcardially with dPBS (Thermo Fisher, MA) followed by 4% paraformaldehyde. The brains were removed from the cranial vault and post fixed in 4% paraformaldehyde overnight at 4°C. Brains were transferred to 15% sucrose overnight at 4°C and subsequently embedded in Richard-Allan Scientific Neg 50™ (ThermoFisher, MA) and then sectioned (30 microns) using a cryostat (Microm HM 550, ThermoFisher, MA).

Sections were collected on superfrost slides (Thermo Scientific, MA), air dried, and fixed with 4% paraformaldehyde for 30 mins and blocked in blocking buffer (2% normal goat serum or rabbit serum and 0.2% triton X-100 in dPBS) for 1 hour at room temperature. Sections were then incubated with primary antibodies for hIGF-1 (Sigma, 1:80 dilution) or GFAP (Sigma, CA, 1:80 dilution), (overnight ~16 hours) followed by a 1 hour incubation with fluorescent-labeled secondary antibodies (Oregon green 488 donkey anti-goat, 1:500 dilution and Oregon green 488 goat anti-rabbit, 1:500 dilution, respectively). Fluorescent labeling was visualized on the Olympus FSX100 Bio Imaging Navigator and captured digitally by FSX-BSW software (Waltham, MA).

### Infarct Analysis

Infarct volume was measured using our previous published procedures (Selvamani and Sohrabji 2010). Two or 5 days after MCAo rats were deeply anesthetized and decapitated, and the brain was rapidly removed. Coronal slices (2 mm thick) between -2.00 mm and +4.00 mm from bregma were sectioned in an adult rat brain slicer matrix (Roboz Surgicals, Gaithersburg, MD) and incubated in a 2% Triphenyl tetrazolium chloride (TTC) solution at 37°C for 20 mins. Stained slices were photographed using an Olympus E950 digital camera attached to a dissecting microscope. Infarct volume was determined from digitized images using the Quantity One software package (Bio-Rad, CA). Typically, 3 such slices were used for analysis. The area of the cortical and striatal infarct was measured separately in all slices, and the area of the entire contralateral hemisphere was also measured. The volume of the infarct was normalized to the volume of the contralateral (non-occluded) hemisphere. To ensure reliable and consistent detection of the infarct zone, images were digitally converted to black and white and magnified. Images were coded and the sections were analyzed by an investigator blind to the code (AO).

### Behavioral analysis

Animals were evaluated for sensorimotor performance pre- and post- stroke using the vibrissae evoked forelimb placing task (Woodlee et al. 2005) as described in (Selvamani and Sohrabji 2010). Animals were subject to same-side placing trials and cross-midline placing trials elicited by stimulating the ipsi- and contra-lesional vibrissae. Same-side placing test: The animal was gently held such that all four limbs were free to move. The animal's ipsi-lesional vibrissae were brushed against the edge of a table to elicit a forelimb placing response, which typically consisted of the forelimb ipsi-lateral to the stimulated vibrissae. Ten trials were performed before the same was repeated for the contra-lesional vibrissae.

**Cross-midline placing test**—The animal was held gently by the upper body such that the ipsi-lesional vibrissae lie perpendicularly to the tabletop and the forelimb on that side is gently restrained as the vibrissae was brushed on the top of the table to evoke a response from the contralateral limb and vice versa. Between each trial, the animal was allowed to rest all four limbs briefly on the tabletop to help relax its muscles. Trials in which the animal seemed to struggle or make premature forelimb movements were not counted.

The vibrissae-elicited forelimb placing test was carried out after AAV5 injection, but before and after MCAo surgeries. An unscored pretest was performed 3 days before MCAo to help acclimatize the animal to the testing procedure. The scored testing schedule was as follows: 2 days prior to the MCAo, 48h (2d after MCAo) and 5d after MCAo. Each testing and pretesting session consisted of 40 trials per animal, 10 trials each for the same-side placing (left and right) and 10 trials each for left and right cross-midline placing. Each trial is rapid and the entire procedure on a single day is approximately 5 min/animal.

Scoring was based on a 4-point scale. A vibrissae-elicited response of the forelimb that included a brisk forward and upward movement that ended in the paw pads making a flat, full contact with the tabletop was scored as 3. If there was a slow or sluggish movement of the limb forward and upward, resulting in just the toes or claws contacting the tabletop, the trial was given a score of 2. When there was a limb movement forward but not upward and the paw made no contact with the tabletop, the trial was scored 1. If the limb did not move in response to stimulation, the trial was given a score 0. Trials scored as a 2 or 3 were counted as a successful placement and the once scored 1 or 0 were considered unsuccessful.

### Neurological Score

A neurological score was obtained based on the following functional tests that were performed 2 days after MCAo. Described below are five tests performed in succession for each animal. For each test, a higher score indicates a more severe deficit.

**Motility Test**—Animals were placed on an open surface and their movement was monitored. Animals that walked normally received a score of 0. Animal with any difficulties were given a 1. Deficits includes immobility, inability to walk straight, circling and falling down (Normal = 0, maximum = 1).

**Grasping**—Animals were suspended by its forelimbs on a small beam. Grasping ability and forelimb strength were assessed. Animals that grasped the beam with both paws were given a 0. Animals that grasped only with the ipsi-lesional paw were given a 1. Animals that could not grasp the beam were given a 2. (Normal = 0, maximum = 2).

**Righting Reflex**—To test the righting reflex, rats were placed on their backs. If the animal took less than 3 seconds to right itself, the animal received a score of 0. An animal that took longer than 3 seconds or was not able to perform the task was given a score of 1. (Normal = 0, maximum = 1)

**Forepaw Disability**—Animals were placed a cylinder and observed. Animals that were able to rear and make contact with the wall of the cylinder with both paws were scored as 0.

Animals that were only able to consistently place the ipsi-lesional paw were scored 1. Animals didn't place either paw in 2 mins, were scored as 2. (Normal = 0, maximum = 2)

**Circling**—Animals with no circling behavior were given a 0. Animals with an inability to walk straight and a flexion of the forelimb towards the paretic side after suspension by the tail were given a score of 1. Animals with constant circling to the paretic side were given a score of 2. Animals with constant circling to the paretic side which a slight tendency to fall were given a score of 3. Animals that were barreling were given a score of 4. Animals that were comatose were given a score of 5. (Normal = 0, maximum = 5)

### Physiological measurements

**Body weight**—Animals were weighed before and after MCAo (2 days) and body weight changes were recorded.

**Systolic Blood Pressure**—Blood pressure was determined by Tail Cuff Blood Pressure Systems (IITC Life Science Inc, CA). Three days prior to baseline testing rats were placed in the apparatus to help acclimatize the animal to the testing environment. A pre-recording was performed 2 days prior to MCAo and a post-surgery recording was performed 2 days after surgery. Each testing and pretesting session consisted of 8 readings per animal, which were averaged.

### Quantitative RT-PCR

**mRNA isolation**—Total RNA was extracted using the Qiagen miReasy kit (Qiagen, CA) from the ischemic and non-ischemic hemispheres as well as astrocytes obtained by magnetic purification from a different set of ischemic and non-ischemic hemispheres. For each sample, 15  $\mu$ L was transferred to a new tube, and 700  $\mu$ L QIAzol lysis reagent was added. Following a 5-min incubation at RT, 140  $\mu$ L chloroform was added to each sample. Following a 2 min incubation at RT, samples were centrifuged at  $12,000 \times g$  for 15 min at  $4^{\circ}\text{C}$ . The aqueous phase was then transferred to a fresh tube and mixed with ethanol (1.5 vol). The sample was then loaded on to an RNeasy Mini Spin Column and centrifuged for 30 seconds at RT,  $13,000 \times g$ . After sequential washes in RWT and RPE buffers, the columns were transferred to a fresh tube and RNA eluted with 50  $\mu$ L of DNase/RNase-free water. Sample purity was assessed by Nanodrop technology and a ratio of 1.8 was considered acceptable. Samples were stored at  $-80^{\circ}\text{C}$  until use.

**Real-time RT-PCR**—mRNA expression for specific genes in AAV5-GFAP-control and AAV5-GFAP-hIGF-1 -treated animals was assessed using real-time qRT-PCR. 200 ng of purified total RNA was used to generate cDNA, using a Universal cDNA Synthesis Kit (Exiqon, Denmark) according to the manufacturer's protocol. 1  $\mu$ L of cDNA samples were used as a PCR reaction template in a 10  $\mu$ L PCR reaction. PCR reactions were run in triplicate on an Applied Biosystems 7900HT real-time PCR instrument (Applied Biosystems, CA) using a SYBR green-based real-time PCR reaction kit (Exiqon, Denmark). 18s mRNA was used as a normalization control. Specificity of the amplification was evaluated by thermal stability analysis of the amplicon. Individual and reference gene primer sets (Integrated DNA Technologies, Coralville, IA) are listed in the Table 1.

## Cell preparation

Animals were anesthetized (xylazine and ketamine i.p.) and perfused intracardially with 100 mL of cold 1X PBS. Ischemic and non-ischemic hemispheres were collected and minced using a blade. Following a wash with X-VIVO 15 (Lonza, TX), a chemically-defined, serum free hematopoietic medium, tissues were first enzymatically dissociated using the Neural Dissociation Kit P (Miltenyi Biotech, CA) and then transferred to a glass Dounce homogenizer and mechanically dissociated. The suspension was then filtered through a 30  $\mu$ m strainer, and washed twice in X-VIVO 15.

**For astrocyte separation**—Cells were incubated with anti-GLAST antibody (1:5) for 10 min. GLAST was selected as a marker because it is an astrocyte-specific, membrane-associated protein and results in a virtually pure astrocyte population (Chisholm et al. 2015). Cells were then washed and spun at  $300 \times g$  for 10 min followed by incubation with biotin microbeads for 15 min. Cells were subsequently washed, spun ( $300 \times g$ ; 10 min), and resuspended in 2 mL of buffer and passed through LS columns. The columns were washed with buffer ( $3 \times 3$  mL), and the flow-through discarded. The LS column was then removed from the magnetic stand. Astrocytes were then eluted from the column and washed in cold dPBS.

**For flow cytometry of immune cells**—The cell pellet retrieved was resuspended in 6 mL of X-VIVO 15, and applied to an Opti-Prep gradient (Axis Shield, Oslo, Norway). The gradient was composed of four 1-mL layers of Opti-prep diluted in X-VIVO 15, arranged in the following order (from bottom to top): 35%, 25%, 20%, and 15%. The 10 mL tube containing the cell suspension and gradient was centrifuged at 1900 RPM for 15 min at 20°C with low acceleration and no brake. Following centrifugation, the top 7 mL of solution containing myelin and debris, was aspirated and discarded. The remaining 3 mL, containing inflammatory cells and glia, was washed twice in X-VIVO 15 and counted (Countess, Life Technologies). The single-cell suspension was then pipetted into three 96-well plates and incubated with conjugated antibodies for the following markers: CD11b, Iba1, CD45, CD86, CD68, CD206, CD163, CD4, CD25, and FoxP3.

For each animal, 2 technical replicates were prepared and phenotyped using a FACSria flow cytometer (BD Biosciences, CA) and analyzed with FlowJo software (Tree Star Inc., OR). The following gating strategy was used to identify microglia/macrophages. First, dead cells and debris was removed from the analysis by gating on forward and side scatter. To control for cellular auto-fluorescence, unstained samples were prepared. Any cells determined to be positive were selected in a gate with  $>1\%$  unstained cells. CD45+ cells were selected and further separated into discrete populations of high, medium, and low based on fluorescence intensity. For macrophages/microphages, after CD45+ positive only cells were selected, an initial gate was scaled to select discrete populations that were positive for both Iba1 and CD11b. For all further analysis, a quadrant system was created so that 99% of the unstained cells were in the third quadrant to determine phenotype and receptor expression. For Tregs, only CD45 high positive cells were used for analysis. An initial gate was scaled to select discrete population positive for CD4. For all further analysis, a quadrant

system was created using CD25 and FoxP3 fluorescence so that 99% of the unstained cells were in the third quadrant to determine phenotype and receptor expression.

### ELISA Assays

**Serum GFAP**—Concentrations of circulating glial fibrillary acidic protein (GFAP) in serum were determined by ELISA (R&D Systems), according to manufacturer's instructions. Briefly, standards, controls, and aliquots of serum samples were loaded into a 96-well plate precoated with antibodies specific for GFAP and incubated at room temperature for 2 hours. With intervening washes, plates were sequentially incubated with 100  $\mu$ L of conjugate for 2 hours, and 100  $\mu$ L of substrate solution for 30 minutes. The color reaction was stopped by an equal volume of stop solution and read at 450 nm in a microplate reader (Bio-Tek, VT). Standard curves were established from optical densities of wells containing known dilutions of standard (1.56 – 100 ng/mL) using KC3 software (Bio-Tek), and sample measurements were interpolated from standard curves. The intraassay coefficient of variation was 1.30%.

**Multiplex Cytokine Kit**—Tissue expression for a panel of cytokine/chemokine was measured in the ischemic and non-ischemic hemisphere and serum of rAAV5-GFAP-hIGF-1 and rAAV5-GFAP-control animals, using a multiplexed magnetic bead immunoassay (Milipore Corp., MA) following manufacturer's instructions. Briefly, the filter plate was blocked with assay buffer for 10 min and decanted. Standards and samples was added into appropriate wells, followed by addition of premixed beads and incubated for 2 hour at room temperature on a plate shaker. Wells were washed 2 times, 25  $\mu$ L of detection antibody was added, incubated for 1 hour incubation at RT and followed by 30 min incubation with addition of 25  $\mu$ L of streptavidin-phycoerythrin per well. After 2 washes, beads were resuspended in 150  $\mu$ L of sheath fluid and a minimum of 50 beads per analyte was analysed in a Bio-Plex suspension array system (Bio-Rad Laboratories, CA). Cytokine/chemokine levels were normalized to total protein content. The following chemokines and cytokines were assessed: Granulocyte colony stimulating factor (G-CSF), eotaxin, GM-CSF, interleukin (IL)-1 $\alpha$ , leptin, macrophage inflammatory protein (MIP)-1a, MIP2, IL-4, IL1-b, IL-2, IL-6, EGF, IL-13, IL-10, IL-12 phosphorylated 70 KDa (IL-12-p-70), Interferon (IFN)- $\gamma$ , IL-5, IL-17A, IL-18, Chemokine C-motif Ligand (CCL2), Interferon gamma induced protein (IP)-10, Growth related oncogene/Keratinocyte derived chemokine (GRO/KC), VEGF, Fractalkine, Lipoploysaccharide-induced CXC (LIX) chemokine, MIP-2, Tumor necrosis factor (TNF)-  $\alpha$ , RANTES (regulated on activation, normal T cell expressed and secreted).

### Statistical analyses

Group size was determined using power analyses. Power analyses was computed based on effect sizes seen in previous data and pilot studies. In order to achieve power of 0.8 (1- $\beta$ ) and Type 1 error rate  $\alpha$ =0.05, the minimum sample size is 4. For these studies, most group sizes ranged from 5 to 8. The Kaplan Maier test was used for survival analysis. For behavioral tests, a paired t-test was used for each group, comparing the values obtained pre- and post-stroke. For all other tests, an unpaired t-test was performed. Group differences were

considered significant at  $p < 0.05$  in each case. The statistical package SPSS (v. 21, IBM) was used for these analyses.

## RESULTS

### Characterization of AAV5 Integration

AAV5 integration was assessed by a combination of histological and molecular techniques. Brain sections from animals injected stereotaxically with either the control (rAAV5-GFAP-hIGF-1; Figure 1A) or the IGF-1 (rAAV5-GFAP-control; Figure 1B) construct were visualized by fluorescent microscopy for the mCherry reporter. The mCherry reporter gene was located downstream of the constitutively expressed cytomegalovirus (CMV) promoter (see Figure 1), hence mCherry expression was widely distributed in neuronal and non-neuronal cells of the cortex (Figure 2Ai) and striatum (Figure 2Aii). mCherry expression was also localized to GFAP-immunolabeled cells (Figure 2B), indicating that the viral construct was internalized to astrocytes. To assess whether the AAV5-GFAP-hIGF-1 construct was functional, sections from AAV5 injected animals were processed for hIGF-1 immunohistochemistry. No hIGF-1 positive cells were seen in animals injected with rAAV5-GFAP-control (Figure 2Ci), while hIGF-1 label (green; Figure 2Cii) was co-localized to mCherry positive cells (red) in the rAAV5-GFAP-hIGF-1 treatment. Many of these double-labeled cells were located around blood vessels.

Expression of hIGF-1 was further confirmed by qRT-PCR in whole brain homogenates and astrocyte homogenates. Astrocytes were collected by GLAST-positive selection by magnetic beads, using our previous procedures that results in a virtually pure astrocyte population (Chisholm et al. 2015). As expected, hIGF-1 was undetectable by qRT-PCR in whole hemisphere homogenates (Figure 2Di) and astrocytes homogenates (Figure 2Dii) from either the ischemic or non-ischemic hemisphere of animals injected with rAAV5-GFAP-control. In contrast, hIGF-1 was highly expressed in whole brain and astrocyte homogenates of the ischemic hemisphere of animals that were injected with AAV-GFAP-hIGF-1, with virtually no hIGF-1 gene expression in the non-ischemic hemisphere. There was no difference in the amount of rat IGF-1 expression in tissue lysates and astrocytes regardless of hemisphere or treatment (Figure 2Diii and 2Div). qRT-PCR of astrocyte homogenates used in these analyses show strong expression of GFAP, and virtually undetectable levels of PECAM (endothelial cell marker) and Iba1 (microglial specific marker) (Figure 2E), indicating an enriched astrocyte population.

### Post-Ischemic Survival

Two doses of AAV5-GFAP-Control and AAV5-GFAP-hIGF-1 were injected into the striatum and cortex, a low dose of  $2.5 \times 10^{11}$  VP/mL and a high dose of  $2.5 \times 10^{12}$  VP/mL. After 6–8 weeks post injection, all animals were subject to MCAo. In the high dose treatment, post-stroke mortality was higher in animals injected with the AAV5-GFAP-control as compared with AAV5-GFAP-hIGF-1 treated animals ( $p < 0.0001$ ; Figure 3A). High dose AAV5-GFAP-control animals did not survive more than 24 hours post-stroke, while high dose AAV5-GFAP-hIGF-1 treated animals survived 5 days, the predetermined termination point for this study.

Animals that received the low dose AAV5 treatment did not show any differences in post-stroke mortality (Figure 3B;  $p = 0.8311$ ). Both rAAV5-GFAP-control and AAV5-GFAP-hIGF-1 groups survived until the predetermined termination point of the study at 5 days. Therefore, all subsequent studies were performed with the low dose AAV5.

### Physiological measures affected by MCAo at the early acute period (2 days) post-stroke

Animals injected with AAV5-GFAP-control and rAAV5-GFAP-hIGF-1 were subject to ischemic stroke for 90 mins followed by reperfusion. Both groups experienced approximately 10% weight loss at 2 days post-stroke, which is commonly seen after stroke, however there was no difference in the extent of weight loss between the two groups (Figure 4A). Systolic blood pressure was also monitored pre- and post-stroke. Pre-stroke, AAV5-GFAP-control animals had a mean systolic blood pressure of 141.8 mmHg, and AAV5-GFAP-hIGF-1 animals averaged 133.9 mmHg. Post-stroke, the mean systolic blood pressure for AAV5-GFAP-control animals significantly decreased 24% to 99.1 mmHg ( $p = 0.0098$ ). The AAV-GFAP-hIGF-1 animals maintained a mean systolic blood pressure of 129.2 mmHg (Figure 4B).

Infarct volume: Infarction was localized largely to the striatum, with smaller cortical infarcts. Infarct volume, assessed at 2 days post stroke, however, was similar between AAV5-GFAP-control and AAV5-GFAP-hIGF-1 groups ( $p = 0.3927$ ; Figure 4C).

The neurological score, an indicator of motor disability, was significantly worse in AAV5-GFAP-control as compared to AAV5-GFAP-hIGF-1 treated animals. Post-stroke, AAV5-GFAP-control animals showed impaired mobility, righting reflex, grasping and pronounced circling behavior resulting in an average neurological score of  $3.86 \pm 0.89$ , which is typical of the post stroke disability observed in middle-aged female rats. 4. In contrast, AAV5-GFAP-hIGF-1 animals had significantly less impairment with an average neurological score of  $2 + 1.0$  ( $p = 0.0033$ ; Figure 4D).

### Post-stroke sensory-motor behavioral outcomes

To assess the effect of AAV5 treatment on sensory motor function post-stroke, the vibrissae evoked-forelimb placing task performance was assessed at 2 days (early acute phase) and 5 days (late acute phase) after MCAo. Consistent with other reports, sensory motor performance improved as animal progressed from the acute phase to the late phase. For the rAAV5-GFAP-control group, there was no response (NR) to either the same side or cross-midline test on the side contralateral to the ischemic side (contralesional) during the early acute phase (Figure 5Ai). In the AAV5-GFAP-hIGF-1 group, during the early acute phase (2d post stroke), post-stroke performance was impaired compared to the pre-stroke performance, however animals in this group were still able to maintain about 45% of their pre-stroke responses to the vibrissae stimulation, unlike the AAV5-GFAP-Control group ( $F_{(3,24)}=3.44$ ;  $p=0.0359$ ; Figure 5Ai).

Similarly, on the ipsilesional side for the early acute phase, AAV5-GFAP-control had no responses to the same side test, while the AAV5-GFAP-hIGF-1 group maintained 40% of their pre-stroke responses ( $F_{(3, 24)} = 13.84$ ;  $p < 0.0001$ ), although these were lower than the

pre-stroke levels ( $F_{(1, 24)} = 50.28$ ;  $p < 0.0001$ ; Figure 5Aii). No loss of response was seen on the cross-midline task on the ipsilesional side.

During the late acute phase (5 days post-stroke), improvement was noted in both groups, however performance in the AAV5-GFAP-control group was significantly worse than pre-stroke levels ( $F_{(1, 14)} = 15.79$ ;  $p = 0.0014$ ). Specifically, AAV5-GFAP-Control animals had lower responses on the same side (54%,  $p = 0.0294$ ) and cross midline (42%,  $p = 0.0059$ ) task on the paw contralateral to the infarct (Figure 5Bi). In contrast, performance of the AAV5-GFAP-hIGF-1 group was statistically no different from the pre-stroke performance ( $p = 0.9$ ; Figure 5Bi and 5 Bii), indicating an improved rate of recovery.

### Blood brain barrier permeability

Circulating levels of GFAP were analyzed as a surrogate measure of blood brain barrier permeability function (Marchi et al. 2004) from serum samples collected pre-stroke, during the early acute and late acute phases of stroke. As shown in Figure 6A, GFAP was detected in all samples, however there was a main effect of stroke (pre and post-stroke) and treatment (AAV-GFAP-Control vs AAV-GFAP-IGF-1). GFAP levels were significantly elevated in both groups after stroke ( $F_{(1,27)} = 7.32$ ,  $p < 0.05$ ), and also significantly elevated by treatment ( $F_{(1,27)} = 7.72$ ,  $p < 0.05$ ) such that animals with AAV-GFAP-hIGF-1 had significantly lower levels of GFAP. Planned comparisons showed that while the groups were no different at baseline, the AAV5-GFAP-hIGF-1 group had almost 50% lower levels of circulating GFAP as compared to the AAV5-GFAP-control group, indicative of decreased blood brain barrier permeability.

### Stroke-induced Inflammation

**Serum Cytokines and Chemokines**—A panel of cytokines and chemokines were examined in serum at 2 days after MCAo for AAV5 treated animals. Almost all cytokines and chemokines were elevated after ischemia (Supplementary Table 1), while a subset were also affected by IGF-1 gene transfer. Compared to the rAAV5-control group (Figure 6B), the AAV5-GFAP-hIGF-1 groups showed elevated levels of G-CSF (main effect of treatment,  $p = 0.0048$ , and stroke,  $p = 0.0331$ ), IL-4 (main effect of treatment,  $p = 0.0332$ , and stroke,  $p = 0.0005$ ), IL-5 (main effect of treatment,  $p = 0.0216$ , and stroke,  $p = 0.0004$ ), Eotaxin (main effect of treatment,  $p = 0.0160$ , and stroke,  $p = 0.0011$ ), and IL12-P70 (main effect of treatment,  $p = 0.0232$ , and stroke,  $p < 0.0001$ ).

**Trafficking of peripheral immune cells**—Flow cytometry was used to determine whether AAV5-GFAP-hIGF-1 affected the cohort of immune cells trafficked to the ischemic hemisphere. Mononuclear cells were harvested from the brain 2 days post-stroke and sorted for cell markers for infiltrating cells. The proportion of infiltrating immune cells identified by high CD45 expression was no different between the AAV5-GFAP-control and AAV5-GFAP-hIGF-1 groups ( $p = 0.4008$ ; Figure 7A). Similarly, there were no group differences between CD4 positive cells ( $p = 0.3950$ ; Figure 7B), however the proportion of infiltrating regulatory T-cells, identified as CD45<sup>high</sup>/CD4/CD25/FoxP3 cells, was significantly elevated in the ischemic hemisphere of AAV5-GFAP-hIGF-1 treated animals as compared to AAV5-GFAP-control animals ( $p = 0.0219$ ; Figure 7C).

In the case of infiltrating macrophages, identified by CD45<sup>high</sup>/CD11b/Iba1, there were no differences in the proportion of these invading cells in the AAV5-GFAP-control and AAV5-GFAP-hIGF-1 groups ( $p = 0.2280$ ; Figure 8A). However, infiltrating macrophages differed in the extent of M1 and M2 cohorts seen in each group. As shown in Fig 8B, the proportion of infiltrating macrophages labeled with CD68/CD86 (M1 phenotype) was decreased by 62% in AAV5-GFAP-IGF-1 treated animals as compared to AAV5-GFAP-control treated animals ( $p = 0.0485$ ). In contrast, the proportion of infiltrating macrophages labeled with CD163/CD206 (M2 phenotype) was increased by 57% in AAV5-GFAP-hIGF-1 treated animals as compared to AAV5-GFAP-control treated animals ( $p = 0.0248$ ; Figure 8C).

There were no group differences in the proportion of resident microglia, identified by CD45<sup>low</sup>/CD11b/Iba1 (data not shown).

### Impact of rAAV5-GFAP-hIGF-1 in a permanent ischemia model

In view of the perivascular location of rAAV-GFAP-hIGF-1 cells, we next determined whether replenishing astrocytic IGF-1 would be effective in a permanent ischemic model (i.e., no reperfusion). As shown in Figure 9, AAV5-GFAP-hIGF-1 treatment had no effect on any of the measures tested. Similar to the transient MCAo, animals lost weight after stroke, and there were no group effects on weight loss (Figure 9A). In case of the neurological score, AAV5-GFAP-control animals were significantly impaired after permanent MCAo (Figure 9B), averaging a score of 4 for both groups, similar to the deficiency seen in the transient MCAo for AAV5-GFAP-control group (compare with Figure 4C). However, in the pMCAo condition, AAV5-GFAP-hIGF-1 treatment had no effect on the neurological score ( $p = 0.9769$ ). Infarct volume (Figure 9C;  $p = 0.7721$ ) was also no different between the two groups, although mean infarct volume was much higher in this model than the transient ischemic model (Figure 4D). The vibrissae evoked forelimb placing task showed that both groups were severely impaired (Figure Ei and Eii), and performance was not improved by AAV5-GFAP-hIGF-1. Overall, AAV5-GFAP-hIGF-1 had no protective effect on the permanent MCAo model.

## Discussion

These data support the hypothesis that elevating IGF-1 expression in astrocytes significantly improves stroke outcomes after transient ischemia-reperfusion in middle-aged female SD rats. AAV5 mediated-expression of hIGF-1 in astrocytes reduced stroke-induced motor impairment, improved sensory motor performance and preferential transmigration of immune cells associated with protective or anti-inflammatory actions. Additionally, systolic blood pressure was stable after transient MCAo in animals with replenished astrocyte IGF-1, while controls experienced a decrease in systolic blood pressure after stroke, which is associated with poorer clinical outcomes and increased mortality in stroke patients (Lin et al. 2015; Okin et al. 2015) especially in the acute period of stroke (Wohlfahrt et al. 2015). These novel findings are in accordance with a growing body of evidence that functional modifications of astrocytes yields major benefits for neurodegenerative diseases (Bajenaru et al. 2002; Furman et al. 2012; Furman et al. 2016).

Age-regulated decreases in the functional capacity of astrocytes may increase the severity of neurological diseases. Aging astrocytes display decreased glucose uptake, GLUT1 expression, and glutathione (GSH) content (Souza et al. 2015), increased levels of intermediate glial fibrillary acidic protein and cytokine secretion (Capilla-Gonzalez et al. 2014; Salminen et al. 2011). Moreover, with age, astrocytes are less sensitive to the anti-inflammatory cytokine IL-10, which results in prolonged neuroinflammation due to persistent microglial activation (Norden et al. 2016). Our previous studies show that, compared to astrocytes from younger female rats, astrocytes from middle-aged females have significantly reduced capacity for glutamate clearance, elevated expression of chemokines and increased ability to recruit PBMC in co-cultures (Lewis et al. 2012). More recent studies show that astrocytes from middle aged females have epigenetic modifications that cause transcriptional repression (Chisholm et al. 2015). This decline in astrocytic functional capacity coincides with an increase in infarct volumes and worsening post-stroke recovery in our model. Whether astrocyte dysfunction is the cause or the result of disease progression has yet to be elucidated. Nevertheless, astrocyte replacement by neural progenitor cells and glial-restricted precursors is reported to have some benefit in acute injury models such as spinal cord injury (Haas and Fischer 2013; van Gorp et al. 2013).

Targeted modification of astrocyte proteins has been used in several neural injury models with success. In Huntington's disease, AAV2/5 mediated restoration of Kir4.1, a rectifying potassium channel, in striatal astrocytes increased longevity and improved motor performance on the rotarod test, footprint analysis, and paw clasp test (Dvorzhak et al. 2016). In spinal cord injury, AAV8-mediated overexpression of Glutamate transporter 1, a protein found primarily in astrocytes, increased diaphragm dysfunction, affected breathing, and increased forelimb dysfunction six weeks after contusion (Li et al. 2014). In hippocampal ischemic injury, heat shock protein (Hsp)70 or superoxide dismutase (SOD) targeted for expression in astrocytes reduced cell death (Xu et al. 2010) *in vivo*, while virally-mediated astrocyte specific expression of the excitatory amino acid transporter (EAAT2) decreased cell death in hippocampal cultures exposed to moderate oxygen glucose deprivation (OGD) (Weller et al. 2008). Interestingly, enhanced expression of EAAT2 was only neuroprotective against moderate levels of OGD but not severe OGD (Weller et al. 2008). This was also seen in the present study where AAV5-mediated IGF-1 in astrocytes improved sensory motor function after stroke in transient MCA (Figure 5) but not permanent MCAo, which results in a much larger infarct volume (Figure 9) and is considered a more severe ischemic injury. In transient focal ischemia, suppression of CD38 in astrocytes reduced transfer of mitochondria, resulting in worse neurological outcomes. (Hayakawa, et. al., 2016). The unique finding of this study is that while non-cell specific viral-mediated transfer of IGF-1 either prior (Zhu et al. 2008) or after (Zhu et al. 2009) MCAo promotes neovascularization and neurogenesis, the present study is first demonstration that astrocyte targeted IGF-1 improves motor outcomes post-stroke.

Surprisingly, while virally-mediated increase in astrocyte IGF-1 improved neurological scores and sensory motor performance and barrier function, it did not lead to reduction of infarct volume. While some studies have shown a significant correlation between increased infarct volume and worse neurological scores and motor impairment (Rogers et al. 1997), other studies showed no correlation between behavioral impairment and infarct volume

(Wahl et al. 1992). Clinically, infarct volumes are not the strongest predictor of long-term prognosis unless combined with NIHSS scores (Baird et al. 2001), as well as involvement of white matter tracts and cerebral blood supply (Heiss and Kidwell 2014). Furthermore, several other growth factors therapies also improve behavior independent of infarct volume. In SD rats, fibroblast growth factor treatment initiated 1 day after MCAo improved behavioral recovery but had no effect on infarct volume (Kawamata et al. 1996). Similarly, rats infused with brain-derived neurotrophic factor after MCAo showed less functional deficit at 28 days after treatment than controls but lesion size measured by T2-MRI did not show differences at 7 and 28 days (Ramos-Cejudo et al. 2015). Additionally, blocking ephrin-A5 signaling, an important pathway for axonal sprouting in premotor and prefrontal motor circuits, in reactive astrocytes after MCAo also improved motor function recovery without a significant change in infarct volume (Overman et al. 2012).

The current studies also reveal a clear difference between the neuroprotective effects of intracerebroventricular (ICV) infusions of hIGF-1 versus AAV5-mediated astrocyte expression of hIGF-1. In middle-aged SD rats, intracerebroventricular (ICV) delivery of hIGF-1 after stroke significantly decreases infarct volume and reduces blood brain barrier permeability (Bake et al. 2014). Furthermore, ICV hIGF-1 treatment decreased trafficking of CD4+ cells and T regulatory cells into the ischemic hemisphere, consistent with the idea that IGF-1 reduces hyperpermeability at the blood brain barrier (Bake et al. 2016). In contrast, astrocyte-derived hIGF-1, did not improve infarct volume although barrier properties were improved as evidenced by serum GFAP levels. Furthermore, astrocyte hIGF-1 did not reduce overall immune trafficking into the ischemic hemisphere, but altered the cohort of immune subtypes. Thus, while there was no difference in the proportion of M1/M2 phenotype resident microglia, infiltrating regulatory T cells and infiltrating M2 macrophages were elevated, indicating that astrocyte-derived hIGF-1 altered immune cell transmigration to favor neuro-supportive and anti-inflammatory cells (Li et al. 2013; Liesz et al. 2015; Won et al. 2015). The difference between the actions of ICV delivery of IGF-1 versus astrocyte mediated hIGF-1 could be due to differences in the amount of IGF-1 available via each method or due to the fact that virally-induced astrocyte hIGF-1 constitutes a 'pretreatment' while ICV-hIGF-1 is a post stroke treatment. Overall, our previous and current data support the hypothesis that the poorer stroke outcomes in older females is associated with age-related decreases in this peptide hormone.

Despite its central location, AAV5-mediated astrocyte hIGF-1 expression has striking effects on the peripheral physiological milieu, as seen by regulation of peripheral cytokines as well as maintenance of systolic blood pressure post-stroke. Astrocytic hIGF-1 elevated circulating levels of granulocyte colony-stimulating factor (GCSF), which is reported to be neuroprotective (Bath and Sprigg 2007; Fan et al. 2015; Shin and Cho 2016), as well as IL-4 and IL-5, which are associated with the Th2 immune response and correlates with reduction in infarct volume (Luo et al. 2015). Peripheral inflammation in stroke patients, usually caused by infection, worsens stroke outcomes (Grau et al. 1999). LPS treatment after stroke, for example, increases macrophage infiltration and caused a prolonged impairment of hindlimb function (Langdon et al. 2010). Thus behavioral improvement seen in AAV-GFAP-hIGF-1 infected animals may be mechanistically linked to a modification of the inflammatory environment.

Astrocytes are the most abundant cell in the brain, outnumbering neurons by at least five to one (Cotrina and Nedergaard 2002; Sofroniew and Vinters 2010). Despite their abundance, stroke research has been mostly neurocentric, aimed towards developing interventions focused on neuronal survival after ischemic injury (Barreto et al. 2011a; Lo et al. 2004), an approach that has not led to successful drug development (Barreto et al. 2011b). The recent trend towards targeting single genes in astrocyte shows promise as a therapy, although most studies have focused on young animal models. Our study is the first to show that correcting a growth factor deficiency in astrocytes in older animals can improve stroke outcomes. In conjunction with refinement of cell based stroke therapies, our data suggest that targeted elevation of IGF-1 in glial-restricted precursors may enhance stroke recovery in older or more susceptible patient populations.

## Supplementary Material

Refer to Web version on PubMed Central for supplementary material.

## Acknowledgments

Supported by NS074895 from the NIH and a Discovery Foundation grant to FS. The authors thank Nihal Salem for expert assistance with qRT-PCR, Miriam Aceves and Mabel Terminal for assistance with flow studies and Dr. Min-Jung Park for assistance with statistical analysis of cytokines.

## References

- Abbott NJ, Ronnback L, Hansson E. Astrocyte-endothelial interactions at the blood-brain barrier. *Nat Rev Neurosci.* 2006; 7:41–53. [PubMed: 16371949]
- Allaman I, Belanger M, Magistretti PJ. Astrocyte-neuron metabolic relationships: for better and for worse. *Trends Neurosci.* 2011; 34:76–87. [PubMed: 21236501]
- Ayadi AE, Zigmond MJ, Smith AD. IGF-1 protects dopamine neurons against oxidative stress: association with changes in phosphokinases. *Exp Brain Res.* 2016; 234:1863–73. [PubMed: 26894890]
- Badan I, Buchhold B, Hamm A, Gratz M, Walker LC, Platt D, Kessler C, Popa-Wagner A. Accelerated glial reactivity to stroke in aged rats correlates with reduced functional recovery. *J Cereb Blood Flow Metab.* 2003; 23:845–54. [PubMed: 12843788]
- Baird AE, Dambrosia J, Janket S, Eichbaum Q, Chaves C, Silver B, Barber PA, Parsons M, Darby D, Davis S, et al. A three-item scale for the early prediction of stroke recovery. *Lancet.* 2001; 357:2095–9. [PubMed: 11445104]
- Bajenaru ML, Zhu Y, Hedrick NM, Donahoe J, Parada LF, Gutmann DH. Astrocyte-specific inactivation of the neurofibromatosis 1 gene (NF1) is insufficient for astrocytoma formation. *Mol Cell Biol.* 2002; 22:5100–13. [PubMed: 12077339]
- Bake S, Okoreeh AK, Alaniz RC, Sohrabji F. Insulin-Like Growth Factor (IGF)-I Modulates Endothelial Blood-Brain Barrier Function in Ischemic Middle-Aged Female Rats. *Endocrinology.* 2016; 157:61–9. [PubMed: 26556536]
- Bake S, Selvamani A, Cherry J, Sohrabji F. Blood Brain Barrier and Neuroinflammation Are Critical Targets of IGF-1-Mediated Neuroprotection in Stroke for Middle-Aged Female Rats. *PLoS ONE.* 2014; 9:e91427. [PubMed: 24618563]
- Bano D, Young KW, Guerin CJ, Lefevre R, Rothwell NJ, Naldini L, Rizzuto R, Carafoli E, Nicotera P. Cleavage of the plasma membrane Na<sup>+</sup>/Ca<sup>2+</sup> exchanger in excitotoxicity. *Cell.* 2005; 120:275–85. [PubMed: 15680332]
- Barreto G, White RE, Ouyang Y, Xu L, Giffard RG. Astrocytes: targets for neuroprotection in stroke. *Cent Nerv Syst Agents Med Chem.* 2011a; 11:164–73. [PubMed: 21521168]

- Barreto GE, Gonzalez J, Torres Y, Morales L. Astrocytic-neuronal crosstalk: implications for neuroprotection from brain injury. *Neurosci Res.* 2011b; 71:107–13. [PubMed: 21693140]
- Bath PM, Sprigg N. Colony stimulating factors (including erythropoietin, granulocyte colony stimulating factor and analogues) for stroke. *Cochrane Database Syst Rev.* 2007;Cd005207. [PubMed: 17443577]
- Bhat R, Crowe EP, Bitto A, Moh M, Katsetos CD, Garcia FU, Johnson FB, Trojanowski JQ, Sell C, Torres C. Astrocyte senescence as a component of Alzheimer's disease. *PLoS One.* 2012; 7:e45069. [PubMed: 22984612]
- Bondy CA, Cheng CM. Signaling by insulin-like growth factor 1 in brain. *Eur J Pharmacol.* 2004; 490:25–31. [PubMed: 15094071]
- Buga AM, Sascau M, Pisoschi C, Herndon JG, Kessler C, Popa-Wagner A. The genomic response of the ipsilateral and contralateral cortex to stroke in aged rats. *J Cell Mol Med.* 2008; 12:2731–53. [PubMed: 18266980]
- Capilla-Gonzalez V, Cebrian-Silla A, Guerrero-Cazares H, Garcia-Verdugo JM, Quinones-Hinojosa A. Age-related changes in astrocytic and ependymal cells of the subventricular zone. *Glia.* 2014; 62:790–803. [PubMed: 24677590]
- Cekanaviciute E, Buckwalter MS. Astrocytes: Integrative Regulators of Neuroinflammation in Stroke and Other Neurological Diseases. *Neurotherapeutics.* 2016; 13:685–701. [PubMed: 27677607]
- Chisholm NC, Henderson ML, Selvamani A, Park MJ, Dindot S, Miranda RC, Sohrabji F. Histone methylation patterns in astrocytes are influenced by age following ischemia. *Epigenetics.* 2015; 10:142–52. [PubMed: 25565250]
- Chisholm NC, Sohrabji F. Astrocytic response to cerebral ischemia is influenced by sex differences and impaired by aging. *Neurobiol Dis.* 2016; 85:245–53. [PubMed: 25843666]
- Cotrina ML, Nedergaard M. Astrocytes in the aging brain. *J Neurosci Res.* 2002; 67:1–10. [PubMed: 11754075]
- Dienel GA, Hertz L. Astrocytic contributions to bioenergetics of cerebral ischemia. *Glia.* 2005; 50:362–88. [PubMed: 15846808]
- Dvorzhak A, Vagner T, Kirmse K, Grantyn R. Functional Indicators of Glutamate Transport in Single Striatal Astrocytes and the Influence of Kir4.1 in Normal and Huntington Mice. *J Neurosci.* 2016; 36:4959–75. [PubMed: 27147650]
- Fan ZZ, Cai HB, Ge ZM, Wang LQ, Zhang XD, Li L, Zhai XB. The Efficacy and Safety of Granulocyte Colony-Stimulating Factor for Patients with Stroke. *J Stroke Cerebrovasc Dis.* 2015; 24:1701–8. [PubMed: 26004861]
- Furman JL, Sama DM, Gant JC, Beckett TL, Murphy MP, Bachstetter AD, Van Eldik LJ, Norris CM. Targeting astrocytes ameliorates neurologic changes in a mouse model of Alzheimer's disease. *J Neurosci.* 2012; 32:16129–40. [PubMed: 23152597]
- Furman JL, Sompol P, Kraner SD, Pleiss MM, Putman EJ, Dunkerson J, Mohmmad Abdul H, Roberts KN, Scheff SW, Norris CM. Blockade of Astrocytic Calcineurin/NFAT Signaling Helps to Normalize Hippocampal Synaptic Function and Plasticity in a Rat Model of Traumatic Brain Injury. *J Neurosci.* 2016; 36:1502–15. [PubMed: 26843634]
- Grau AJ, Buggle F, Schnitzler P, Spiel M, Lichy C, Hacke W. Fever and infection early after ischemic stroke. *J Neurol Sci.* 1999; 171:115–20. [PubMed: 10581377]
- Haas C, Fischer I. Human astrocytes derived from glial restricted progenitors support regeneration of the injured spinal cord. *J Neurotrauma.* 2013; 30:1035–52. [PubMed: 23635322]
- Hayakawa K, Esposito E, Wang X, Terasaki Y, Liu Y, Xing C, Ji X, Lo EH. Transfer of mitochondria from astrocytes to neurons after stroke. *Nature.* 2016; 535:551–5. [PubMed: 27466127]
- Heiss WD, Kidwell CS. Imaging for prediction of functional outcome and assessment of recovery in ischemic stroke. *Stroke.* 2014; 45:1195–201. [PubMed: 24595589]
- Jezierski MK, Sohrabji F. Neurotrophin expression in the reproductively senescent forebrain is refractory to estrogen stimulation. *Neurobiol Aging.* 2001; 22:309–19. [PubMed: 11182481]
- Karki P, Smith K, Johnson J Jr, Lee E. Astrocyte-derived growth factors and estrogen neuroprotection: role of transforming growth factor-alpha in estrogen-induced upregulation of glutamate transporters in astrocytes. *Mol Cell Endocrinol.* 2014; 389:58–64. [PubMed: 24447465]

- Kawamata T, Alexis NE, Dietrich WD, Finklestein SP. Intracisternal basic fibroblast growth factor (bFGF) enhances behavioral recovery following focal cerebral infarction in the rat. *J Cereb Blood Flow Metab.* 1996; 16:542–7. [PubMed: 8964792]
- Langdon KD, MacLellan CL, Corbett D. Prolonged, 24-h delayed peripheral inflammation increases short- and long-term functional impairment and histopathological damage after focal ischemia in the rat. *Journal of Cerebral Blood Flow and Metabolism: Official Journal of the International Society of Cerebral Blood Flow and Metabolism.* 2010; 30:1450–1459.
- Latour A, Grintal B, Champeil-Potokar G, Hennebelle M, Lavielle M, Dutar P, Potier B, Billard JM, Vancassel S, Denis I. Omega-3 fatty acids deficiency aggravates glutamatergic synapse and astroglial aging in the rat hippocampal CA1. *Aging Cell.* 2013; 12:76–84. [PubMed: 23113887]
- Lewis DK, Thomas KT, Selvamani A, Sohrabji F. Age-related severity of focal ischemia in female rats is associated with impaired astrocyte function. *Neurobiol Aging.* 2012; 33:1123, e1–16.
- Li K, Nicaise C, Sannie D, Hala TJ, Javed E, Parker JL, Putatunda R, Regan KA, Suain V, Brion JP, et al. Overexpression of the astrocyte glutamate transporter GLT1 exacerbates phrenic motor neuron degeneration, diaphragm compromise, and forelimb motor dysfunction following cervical contusion spinal cord injury. *J Neurosci.* 2014; 34:7622–38. [PubMed: 24872566]
- Li P, Gan Y, Sun BL, Zhang F, Lu B, Gao Y, Liang W, Thomson AW, Chen J, Hu X. Adoptive regulatory T-cell therapy protects against cerebral ischemia. *Ann Neurol.* 2013; 74:458–71. [PubMed: 23674483]
- Liesz A, Hu X, Kleinschnitz C, Offner H. Functional role of regulatory lymphocytes in stroke: facts and controversies. *Stroke.* 2015; 46:1422–30. [PubMed: 25791715]
- Lin MP, Ovbiagele B, Markovic D, Towfighi A. Systolic blood pressure and mortality after stroke: too low, no go? *Stroke.* 2015; 46:1307–13. [PubMed: 25765723]
- Lo EH, Broderick JP, Moskowitz MA. tPA and proteolysis in the neurovascular unit. *Stroke.* 2004; 35:354–6. [PubMed: 14757877]
- Lo EH, Dalkara T, Moskowitz MA. Mechanisms, challenges and opportunities in stroke. *Nat Rev Neurosci.* 2003; 4:399–415. [PubMed: 12728267]
- Luo Y, Zhou Y, Xiao W, Liang Z, Dai J, Weng X, Wu X. Interleukin-33 ameliorates ischemic brain injury in experimental stroke through promoting Th2 response and suppressing Th17 response. *Brain Res.* 2015; 1597:86–94. [PubMed: 25500143]
- Madathil SK, Carlson SW, Brelsfoard JM, Ye P, D’Ercole AJ, Saatman KE. Astrocyte-Specific Overexpression of Insulin-Like Growth Factor-1 Protects Hippocampal Neurons and Reduces Behavioral Deficits following Traumatic Brain Injury in Mice. *PLoS One.* 2013; 8:e67204. [PubMed: 23826235]
- Manwani B, Liu F, Xu Y, Persky R, Li J, McCullough LD. Functional recovery in aging mice after experimental stroke. *Brain Behav Immun.* 2011; 25:1689–700. [PubMed: 21756996]
- Marchi N, Cavaglia M, Fazio V, Bhudia S, Hallene K, Janigro D. Peripheral markers of blood–brain barrier damage. *Clinica Chimica Acta.* 2004; 342:1–12.
- Mozaffarian D, Benjamin EJ, Go AS, Arnett DK, Blaha MJ, Cushman M, de Ferranti S, Després J-P, Fullerton HJ, Howard VJ, et al. Heart Disease and Stroke Statistics—2015 Update. A Report From the American Heart Association. 2015; 131:e29–e322.
- Norden DM, Trojanowski PJ, Walker FR, Godbout JP. Insensitivity of astrocytes to interleukin 10 signaling following peripheral immune challenge results in prolonged microglial activation in the aged brain. *Neurobiol Aging.* 2016; 44:22–41. [PubMed: 27318131]
- Okin PM, Kjeldsen SE, Devereux RB. Systolic Blood Pressure Control and Mortality After Stroke in Hypertensive Patients. *Stroke.* 2015; 46:2113–8. [PubMed: 26089332]
- Olsen ML, Sontheimer H. Functional implications for Kir4.1 channels in glial biology: from K(+) buffering to cell differentiation. *Journal of neurochemistry.* 2008; 107:589–601. [PubMed: 18691387]
- Overman JJ, Clarkson AN, Wanner IB, Overman WT, Eckstein I, Maguire JL, Dinov ID, Toga AW, Carmichael ST. A role for ephrin-A5 in axonal sprouting, recovery, and activity-dependent plasticity after stroke. *Proc Natl Acad Sci U S A.* 2012; 109:E2230–9. [PubMed: 22837401]
- Panickar KS, Norenberg MD. Astrocytes in cerebral ischemic injury: morphological and general considerations. *Glia.* 2005; 50:287–98. [PubMed: 15846806]

- Posada-Duque RA, Barreto GE, Cardona-Gomez GP. Protection after stroke: cellular effectors of neurovascular unit integrity. *Front Cell Neurosci.* 2014; 8:231. [PubMed: 25177270]
- Ramos-Cejudo J, Gutiérrez-Fernández M, Otero-Ortega L, Rodríguez-Frutos B, Fuentes B, Vallejo-Cremades MT, Hernanz TN, Cerdán S, Díez-Tejedor E. Brain-Derived Neurotrophic Factor Administration Mediated Oligodendrocyte Differentiation and Myelin Formation in Subcortical Ischemic Stroke. *Stroke.* 2015; 46:221–228. [PubMed: 25395417]
- Ridet JL, Malhotra SK, Privat A, Gage FH. Reactive astrocytes: cellular and molecular cues to biological function. *Trends Neurosci.* 1997; 20:570–7. [PubMed: 9416670]
- Rogers DC, Campbell CA, Stretton JL, Mackay KB. Correlation Between Motor Impairment and Infarct Volume After Permanent and Transient Middle Cerebral Artery Occlusion in the Rat. *Stroke.* 1997; 28:2060–2066. [PubMed: 9341719]
- Rossi DJ, Brady JD, Mohr C. Astrocyte metabolism and signaling during brain ischemia. *Nat Neurosci.* 2007; 10:1377–1386. [PubMed: 17965658]
- Salminen A, Ojala J, Kaarniranta K, Haapasalo A, Hiltunen M, Soininen H. Astrocytes in the aging brain express characteristics of senescence-associated secretory phenotype. *Eur J Neurosci.* 2011; 34:3–11. [PubMed: 21649759]
- Selvamani A, Sohrabji F. The neurotoxic effects of estrogen on ischemic stroke in older female rats is associated with age-dependent loss of IGF-1. *The Journal of neuroscience : the official journal of the Society for Neuroscience.* 2010; 30:6852–6861. [PubMed: 20484627]
- Shin YK, Cho SR. Exploring Erythropoietin and G-CSF Combination Therapy in Chronic Stroke Patients. *Int J Mol Sci.* 2016; 17:463. [PubMed: 27043535]
- Sofroniew MV, Vinters HV. Astrocytes: biology and pathology. *Acta Neuropathol.* 2010; 119:7–35. [PubMed: 20012068]
- Souza DG, Bellaver B, Raupp GS, Souza DO, Quincozes-Santos A. Astrocytes from adult Wistar rats aged in vitro show changes in glial functions. *Neurochem Int.* 2015; 90:93–7. [PubMed: 26210720]
- Topp KS, Faddis BT, Vijayan VK. Trauma-induced proliferation of astrocytes in the brains of young and aged rats. *Glia.* 1989; 2:201–11. [PubMed: 2526082]
- Utada K, Ishida K, Tohyama S, Urushima Y, Mizukami Y, Yamashita A, Uchida M, Matsumoto M. The combination of insulin-like growth factor 1 and erythropoietin protects against ischemic spinal cord injury in rabbits. *J Anesth.* 2015; 29:741–8. [PubMed: 26003536]
- van Gorp S, Leerink M, Kakinohana O, Platoshyn O, Santucci C, Galik J, Joosten EA, Hruska-Plochan M, Goldberg D, Marsala S, et al. Amelioration of motor/sensory dysfunction and spasticity in a rat model of acute lumbar spinal cord injury by human neural stem cell transplantation. *Stem Cell Res Ther.* 2013; 4:57. [PubMed: 23710605]
- Wahl F, Allix M, Plotkine M, Boulu RG. Neurological and behavioral outcomes of focal cerebral ischemia in rats. *Stroke.* 1992; 23:267–72. [PubMed: 1561657]
- Weller ML, Stone IM, Goss A, Rau T, Rova C, Poulsen DJ. Selective Over Expression Of EAAT2 In Astrocytes Enhances Neuroprotection From Moderate But Not Severe Hypoxia-Ischemia. *Neuroscience.* 2008; 155:1204–1211. [PubMed: 18620031]
- Wohlfahrt P, Krajcoviechova A, Jozifova M, Mayer O, Vanek J, Filipovsky J, Cifkova R. Low blood pressure during the acute period of ischemic stroke is associated with decreased survival. *J Hypertens.* 2015; 33:339–45. [PubMed: 25380168]
- Won S, Lee JK, Stein DG. Recombinant tissue plasminogen activator promotes, and progesterone attenuates, microglia/macrophage M1 polarization and recruitment of microglia after MCAO stroke in rats. *Brain Behav Immun.* 2015; 49:267–79. [PubMed: 26093305]
- Woodlee MT, Asseo-Garcia AM, Zhao X, Liu SJ, Jones TA, Schallert T. Testing forelimb placing “across the midline” reveals distinct, lesion-dependent patterns of recovery in rats. *Exp Neurol.* 2005; 191:310–7. [PubMed: 15649486]
- Xie L, Yang SH. Interaction of astrocytes and T cells in physiological and pathological conditions. *Brain Res.* 2015; 1623:63–73. [PubMed: 25813828]
- Xu L, Emery JF, Ouyang YB, Voloboueva LA, Giffard RG. Astrocyte targeted overexpression of Hsp72 or SOD2 reduces neuronal vulnerability to forebrain ischemia. *Glia.* 2010; 58:1042–9. [PubMed: 20235222]

- Zhu W, Fan Y, Frenzel T, Gasmi M, Bartus RT, Young WL, Yang GY, Chen Y. Insulin growth factor-1 gene transfer enhances neurovascular remodeling and improves long-term stroke outcome in mice. *Stroke*. 2008; 39:1254–61. [PubMed: 18309153]
- Zhu W, Fan Y, Hao Q, Shen F, Hashimoto T, Yang G-Y, Gasmi M, Bartus RT, Young WL, Chen Y. Postischemic IGF-1 gene transfer promotes neurovascular regeneration after experimental stroke. *Journal of cerebral blood flow and metabolism : official journal of the International Society of Cerebral Blood Flow and Metabolism*. 2009; 29:1528–1537.

Author Manuscript

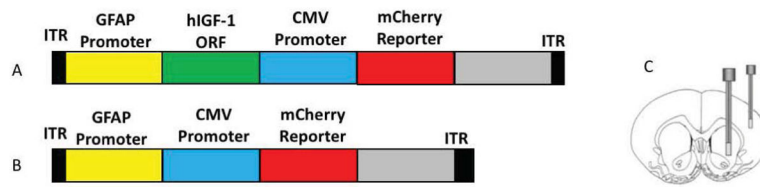
Author Manuscript

Author Manuscript

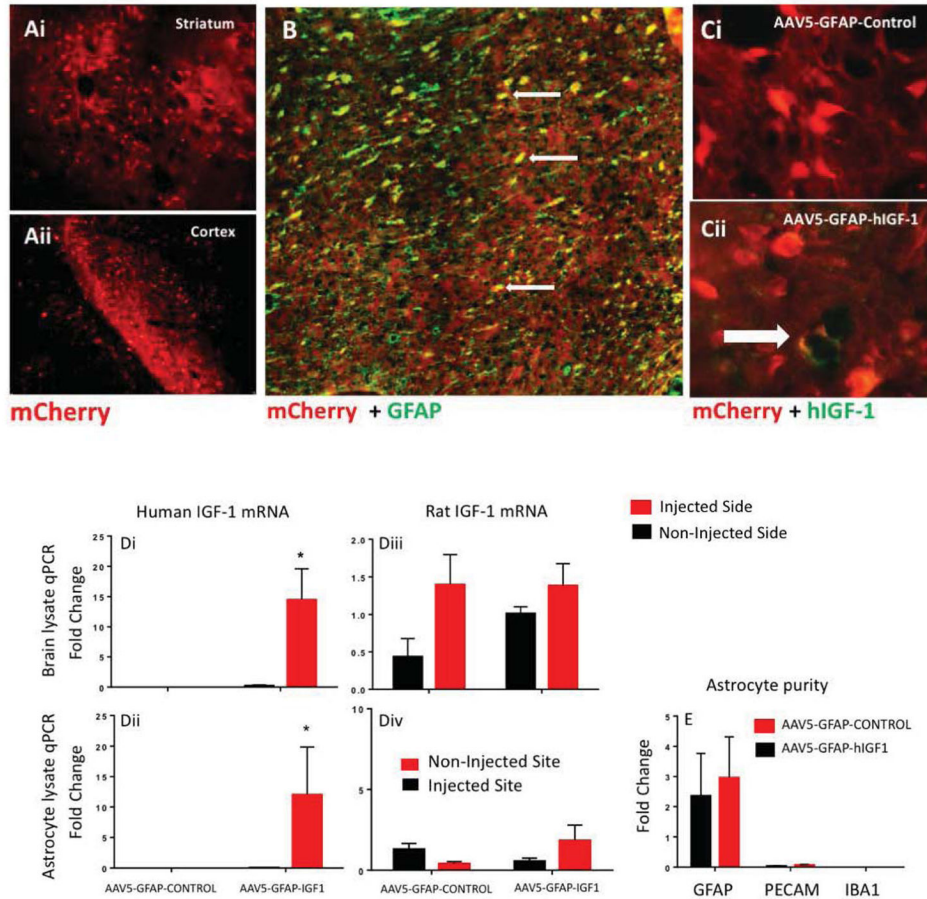
Author Manuscript

**Main points**

1. Ischemia-induced damage and disability is worse in middle-aged female rats than young female rats.
2. Astrocyte-specific gene transfer of IGF-1 improves the immunological response and motor sensory recovery after stroke in middle-aged females.

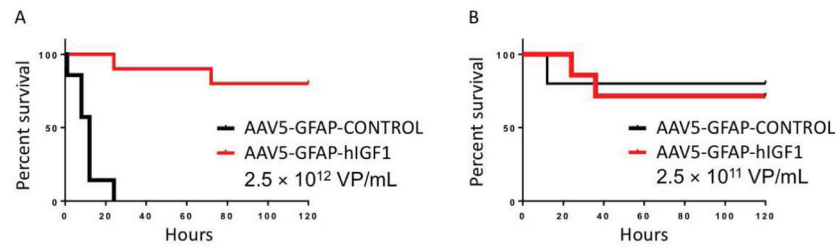
**Figure 1. AAV5 constructs**

Schematic representations of the AAV serotype 5 viral constructs for AAV5-GFAP-hIGF-1 (1A) and AAV5-GFAP-control (1B). (C.) AAV5 virus was injected into the cortex and the striatum on the same hemisphere.



### Figure 2. Integration of the AAV5 in brain

AAV5 uptake into cells was detected by the mCherry reporter. A) At the striatal (Ai) and cortical (Aii) injection sites, both glial and neuronal cells were labeled by the mCherry reporter. B) Immunohistochemical labeling of GFAP in green and AAV5 mCherry reporter in red. Arrows indicate cells that are double labeled for AAV5 mCherry reporter and the glia marker GFAP. C) Immunohistochemistry for hIGF1 in green and AAV5 mCherry reporter in red. hIGF-1 positive cells were seen in animals injected with AAV5-GFAP-hIGF-1 (Cii) but not the AAV5-GFAP-control injected animals (Ci). hIGF-1 positive cells were colocalized to mCherry-labeled cells and mainly seen around blood vessels. D) mRNA expression of human and rat IGF-1 in harvested astrocytes. mRNA hIGF-1 expression was significantly only increased in the injected hemisphere site in whole brain (Di) and in harvested astrocytes (Dii). (N=5–8). No differences were seen in rat IGF-1 mRNA in whole brain lysates (N=4) (Diii) or astrocyte mRNA (N=6–8) (Div). Magnetically harvested astrocytes produced a virtually pure population (E). ( $F_{(2, 18)} = 7.132$   $P = 0.0052$  Two-way ANOVA) (All graphs represent mean  $\pm$  SEM)

**Figure 3. Post-ischemic survival**

Kaplan–Meier Survival Analysis for High Dose and Lose Dose. A) Animals who received the high dose AAV5-GFAP-hIGF-1 had significant survival post-stroke over 120 hours (5 days) compared to high dose AAV5-GFAP-control ( $p < 0.0001$ ;  $n = 7-10$ ) B) Animals that received the lose dose AAV5-GFAP-hIGF-1 or AAV5-GFAP-control construct did not show differences in post-stroke survival over 120 hours ( $p = 0.8311$ ) ( $N = 4 - 5$ )

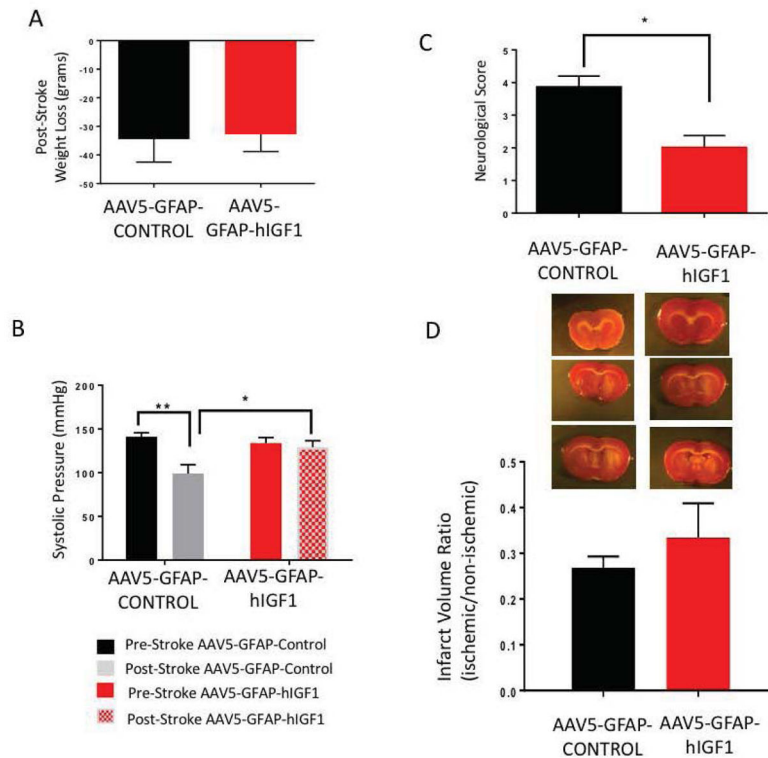


**Figure 4. Low dose post-ischemic outcomes**

A) No differences were seen between AAV5-GFAP-hIGF-1 and AAV5-GFAP-control treated animals in weight loss after stroke. (Unpaired t test;  $p=0.8675$ ) B) AAV5-GFAP-hIGF-1 treatment preserved systolic blood pressure. ( $F(1, 12) = 6.012$ ,  $P = 0.0305$ ; post hoc t-test for pre- and post-AAV5-GFAP-Control  $p = 0.0042$ ). C) Neurological deficits were significantly decreased in the AAV5-GFAP-hIGF-1 animals as compared to the controls (unpaired t test;  $p = 0.0033$ ). D) No differences found in infarct volumes between groups (unpaired t test;  $p = 0.3927$ ) ( $N = 7 - 8$ ). All graphs represent mean  $\pm$  SEM.

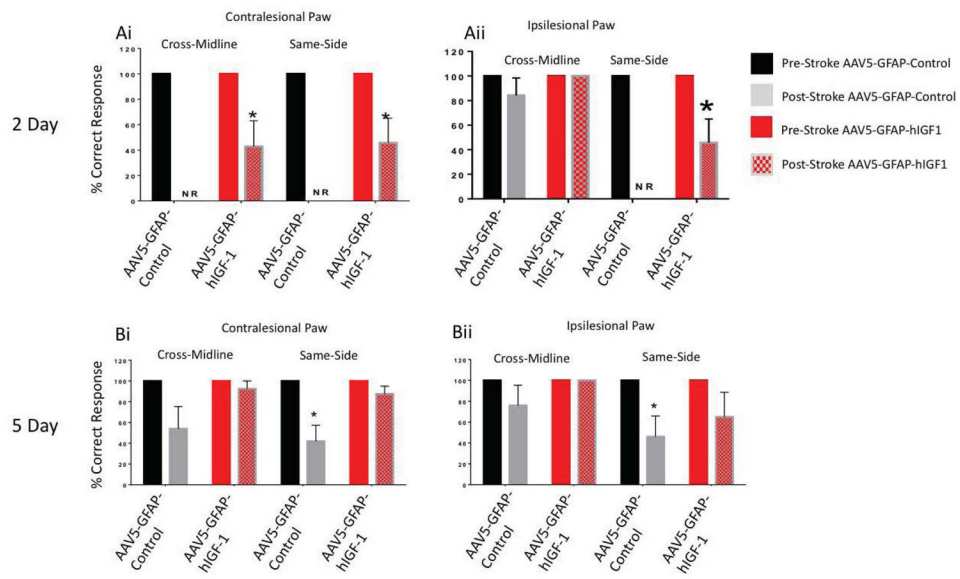


### Figure 5. Vibrissae-Evoked Forelimb Placing Test

Sensory motor performance was evaluated by vibrissae-evoked forelimb placing task at 2 days (Ai and Aii) and 5 days (Bi and Bii) after stroke. Histogram depicts percent (+SEM) correct responses over 10 trials for tests of the contralateral (Ai and Bi) and ipsilateral (Aii and Bii) paw. NR: No Response; \*:  $p < 0.05$ ,  $n = 7-8$  for 2d post stroke,  $n = 4-5$  at 5d post stroke.

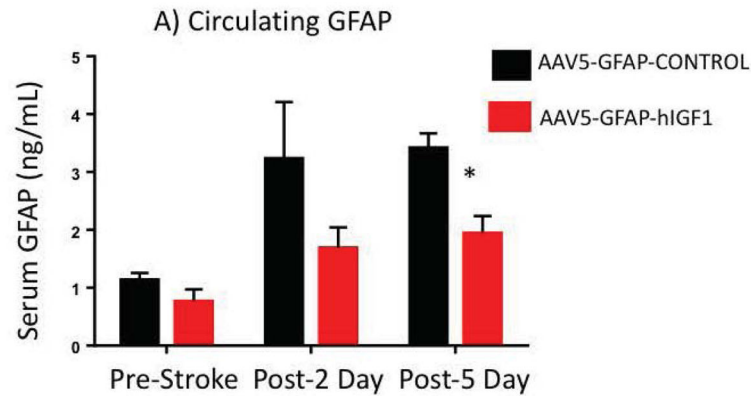
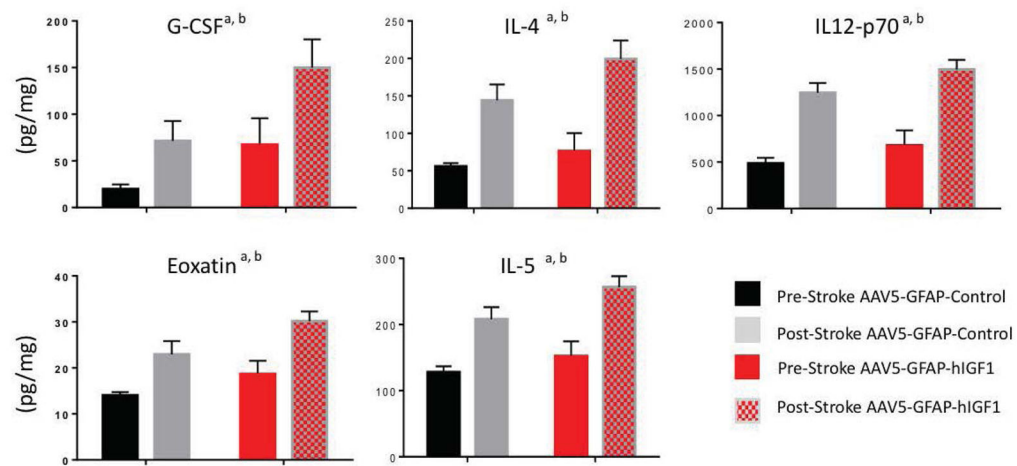
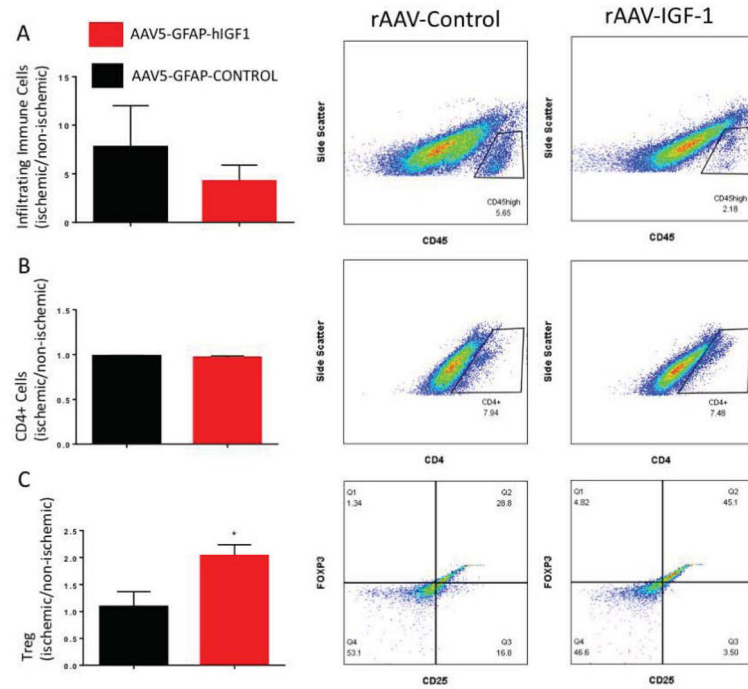


Figure 6B

**Figure 6. Serum Analysis**

A) GFAP serum levels measured pre-stroke and at 2d and 5d post stroke in samples from AAV5-GFAP-control and AAV5-GFAP-hIGF-1 animals. a: main effect of AAV treatment; b: main effect of stroke, \*:  $p > 0.05$ ;  $n = 6-7$ . B) Cytokine levels of AAV5-GFAP-control and AAV5-GFAP-hIGF-1 animals in serum samples taken pre-stroke and 2 days post stroke for G-CSF, IL-4, IL-12-p70, Eotaxin, and IL-5. (a: main effect of treatment; b: main effect of stroke) All graphs represent mean  $\pm$  SEM.  $N = 6-7$  in each group.



### Figure 7. Infiltrating regulatory T-cell Analysis

A) Proportion of (CD45<sup>high</sup>) infiltrating immune cells detected in AAV5-GFAP-control and AAV5-GFAP-hiGF-1 treated animals ( $p = 0.4008$ ). B) Proportion of CD4<sup>+</sup> cells in AAV5-GFAP-control and AAV5-GFAP-hiGF-1 treated animals ( $p = 0.3950$ ). C) Proportion of infiltrating regulatory T-cells (CD45<sup>high</sup>, CD4/CD25/FoxP3) in AAV5-GFAP-control and AAV5-GFAP-hiGF-1 treated animals ( $p = 0.0219$ ). All graphs represent mean  $\pm$  SEM,  $n = 5-6$  in each group.

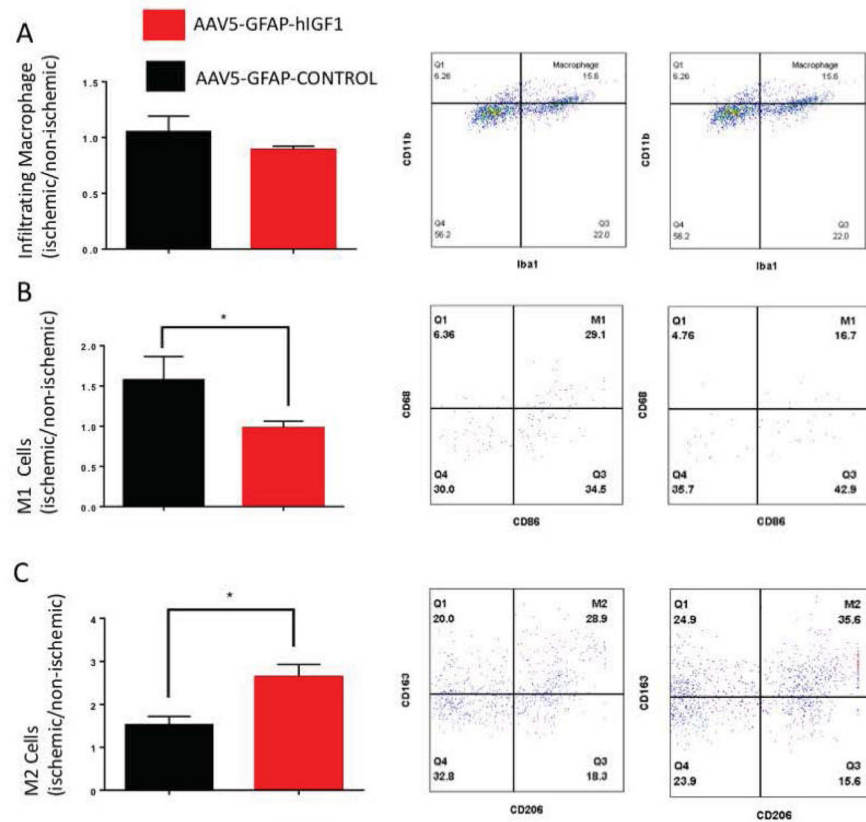


### Figure 8. Infiltrating M1/M2 Macrophage Analysis

A) Proportion of CD45<sup>high</sup>/CD11b/Iba1 stained cells (infiltrating macrophages) in AAV5-GFAP-control and AAV5-GFAP-hIGF-1 treated animals ( $p = 0.2280$ ). B) Proportion of infiltrating M1 macrophages (CD45<sup>high</sup>/CD11b/Iba1/CD68/CD86 stained cells) in AAV5-GFAP-control and AAV5-GFAP-hIGF-1 treated animals (\*:  $p = 0.0485$ ) and infiltrating M2 macrophages (CD45<sup>high</sup>/CD11b/Iba1/CD163/CD206) (\*:  $p = 0.0248$ ). All graphs represent mean  $\pm$  SEM,  $n = 5-6$  in each group.

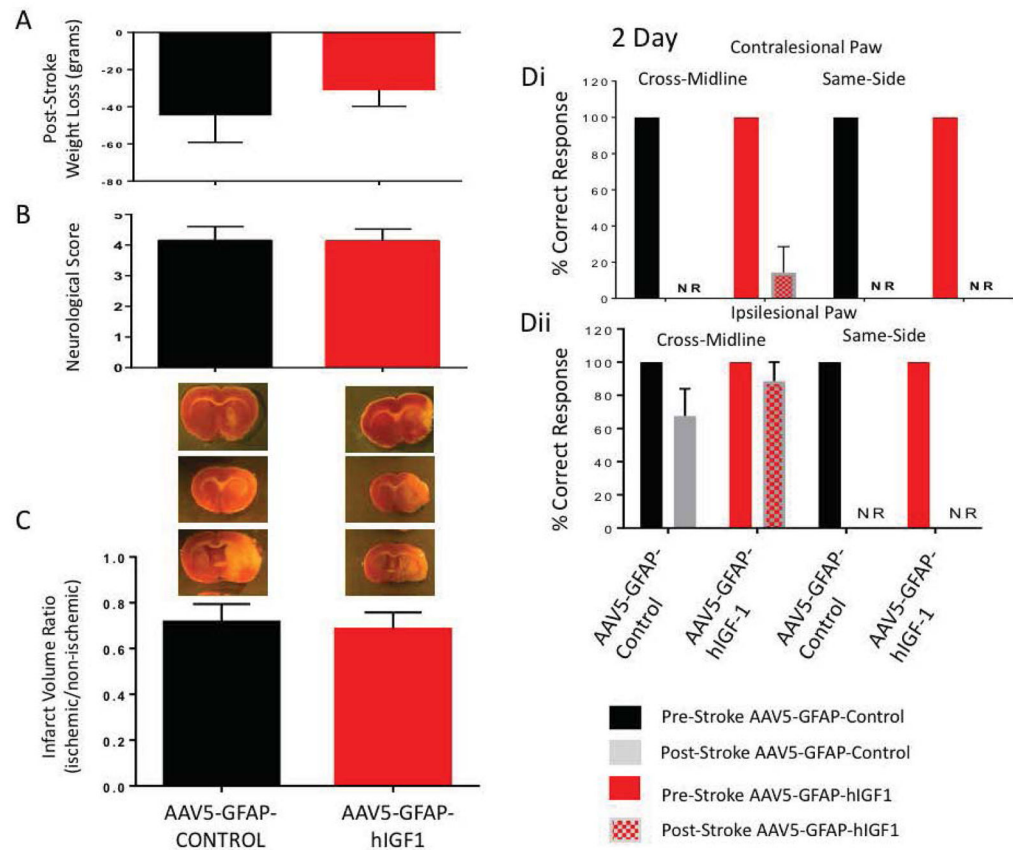


**Figure 9. Permanent MCAo Model**

A) Weight loss due to stroke in AAV5-GFAP-control and AAV5-GFAP-hIGF-1 treated animals. B) Neurological score assessed 2 days after stroke in AAV5-GFAP-control and AAV5-GFAP-hIGF-1 treated animals. C) Infarct volume measured 5 days after stroke in AAV5-GFAP-control and AAV5-GFAP-hIGF-1 treated animals. Di and Dii) Sensory-motor performance measured by vibrissae evoked forelimb placing task in AAV5-GFAP-control and AAV5-GFAP-hIGF-1 treated animals. All graphs represent mean  $\pm$  SEM.  $n = 5-6$  in each group. No significant differences were seen in any of these measures.

**Table 1**

Gene Name	Forward Primer	Reverse Primer
Human IGF-1	AGATGCACACCATGCCTCC	CATCCACGATGCCTGTCTGA
Rat IGF-1	GCTGGTGGACGCTCTTCAGT	TTCAGCGGAGCACAGTACAT
GLAST	AATGAAGCCATCATGAGATTGGT	CCCTGCGATCAAGAAGAGGAT
GFAP	GGTGGAGAGGGACAATCTCA	CCAGCTGCTCCTGGAGTTCT
Iba1	CCATGAAGCCTGAGGAAATTCA	TTATATCCACCTCCAATTAGGGCA
PECAM	TTGTGACCAGTCTCCGAAGC	TGGCTGTTGGTTCCACACT
18S	ATGGCCGTCTTAGTTGGTG	CGCTGAGCCAGTCAGTGTAG

Author Manuscript

Author Manuscript

Author Manuscript

Author Manuscript